

Novel structures and collapse of solitons in nonminimally gravitating dark matter halos

Jiajun Chen^a and Hong-Yi Zhang^{b,*}

^aSchool of Physical Science and Technology, Southwest University, Chongqing 400715, China

^bTsung-Dao Lee Institute & School of Physics and Astronomy, Shanghai Jiao Tong University, Shanghai 201210, China

E-mail: chenjiajun@swu.edu.cn, hongyi18@sjtu.edu.cn

Abstract. Ultralight dark matter simulations predict condensates with short-range correlation, known as solitons or boson stars, at the centers of dark matter halos. This paper investigates the formation and collapse of dark matter solitons influenced by nonminimal gravitational effects, characterized by gradient-dependent self-interactions of dark matter and an additional source in Poisson's equation for gravity. Our simulations suggest that the initial evolution of dark matter resembles that without nonminimal gravitational effects. However, regions with negative potential curvature may develop, and solitons will collapse when their densities reach certain critical values for both positive and negative coupling constants. With strong nonminimal gravitational effects, we verify that linear density perturbations could grow on both large and small scales, potentially enhancing structure formation.

*Corresponding author.

Contents

1	Introduction	1
2	Field equations and numerical setup	2
3	Formation and collapse of solitons in dark matter halos	4
3.1	Condensation of self-gravitating solitons	4
3.2	Nonminimally gravitating solitons	5
3.3	Dark matter with positive nonminimal couplings	5
3.4	Dark matter with negative nonminimal couplings	8
4	Conclusions	9

1 Introduction

A popular idea of dark matter involves a sub-eV scalar field known as ultralight dark matter [1–4]. This class of models can produce cosmological structures similar to cold dark matter on large scales [5, 6]. On small scales, the thermalization of scalar particles typically leads to the formation of condensations with short-range correlations called solitons or boson stars [7, 8]. Focusing on the very light end of the mass spectrum $\mathcal{O}(10^{-22}\text{--}10^{-20})\text{eV}$, simulations in both expanding and nonexpanding backgrounds show that solitons emerge at the centers of dark matter halos [9–21]. Solitons exhibit flat and smooth central density profiles, offering a natural solution to the discrepancy between the cuspy density profiles predicted by cold dark matter simulations and the flatter ones observed in galactic centers [2]. Ultralight dark matter is also proposed as a solution to the final parsec problem in simulations of supermassive black hole mergers [22]. In these simulations, inspirals stall at a few parsecs apart due to insufficient gravitational wave emission for orbits on those scales, which is problematic given the abundance of very massive black holes observed at galactic centers. However, orbiting near a solitonic core [23] or interacting with ultralight dark matter granules [24] could provide mechanisms to facilitate orbital decay.¹

Solitons give rise to important opportunities for discovering and constraining ultralight dark matter. For examples, solitons might dominate the bulge dynamics in massive galaxies and could potentially represent the majority of halo mass in smaller dwarf galaxies. Analysis against observed galactic kinematics has provided strong constraints on DM mass and self-interactions [31–42]. If dark matter is coupled to photons, solitons could generate observable electromagnetic signals [43–47].

Therefore, a detailed understanding about the formation and growth of solitons is crucial for inferring their cosmological abundance. In the simplest scenario, where dark matter interacts only through minimal couplings to gravity, solitons can condense from a thermal bath of dark matter particles through kinetic relaxation [48]. They continue to grow until relativistic effects become important. It is suggested that soliton growth slows once they become massive enough to heat the surrounding halo [13, 17], with the masses of the soliton M_s and the halo M_h approximately following the scaling $M_s \propto M_h^{1/3}$. However, there is

¹Other potential solutions to the final parsec problem involve, for example, self-interacting dark matter [25], accretion disks [26–28], or axisymmetric galactic halo profile [29] (which was debated in [30]).

ongoing debate about the quantitative characterization of the soliton growth rate [10, 13, 17, 49, 50]. Baryonic matter could influence this process, typically leading to more compact cores [51, 52].

As dense clumps of particles, dark matter densities within solitons could be many orders of magnitude higher than the local density $\sim 0.4\text{GeV}/\text{cm}^3$ inferred from galactic rotation curves [53, 54]. This implies that solitons are likely to be influenced by dark matter self-interactions and the foregoing simple picture needs to be improved. These self-interactions, to the leading order in the nonrelativistic limit, are quartic in fields (cubic terms are not allowed since a single nonrelativistic particle cannot create two nonrelativistic particles and vice versa). In the case of axions—hypothetical particles proposed to explain the absence of the neutron electric dipole moment [55–57]—attractive self-interactions can destabilize solitons when their mass exceeds a threshold [8, 58–64], resulting in bursts of relativistic axions [65]. On the other hand, soliton condensation could be promoted by repulsive self-interactions [17], which can arise from spontaneous symmetry breaking and integrating out heavy degrees of freedom [66].

Dark matter self-interactions can also result from their nonminimal couplings to curvature fields such as $\xi\phi^2R/2$, where ϕ is a scalar dark matter field, R is the Ricci scalar, and ξ characterizes the coupling strength [8, 67].² This leading-order nonminimal gravitational interaction (NGI) manifest as quartic terms in fields, including both gradient-independent and gradient-dependent parts. At first glance, the gradient-dependent part seems negligible due to the suppression by the small momenta of particles, reducing the effective self-interactions to the traditional parameterization used in previous references. However, as shown in [8], these two components are interrelated because they arise from integrating out the nonlocal gravitational potential, described by a modified Poisson’s equation. In this paper, we aim to investigate the impact of this new component of self-interactions on the formation and growth of solitons using 3+1-dimensional simulations. We will see that regions with negative mass density (defined as the source of the Poisson’s equation) could develop. By tracking the evolution of maximum densities, we demonstrate that gradient-dependent self-interactions impose an upper bound on the mass of solitons for both positive and negative couplings, thereby affecting the mass distribution of solitons in the long-term evolution.

The rest of the paper is organized as follows. In section 2, we introduce the key components of nonminimally gravitating dark matter and outline our numerical strategy. The results of our simulations are presented in section 3. First, we reproduce the numerical evolution of dark matter without NGIs in section 3.1. Next, we discuss key properties of nonminimally gravitating solitons based on theoretical arguments in 3.2. The evolution of nonminimally gravitating dark matter with positive and negative couplings is analyzed in sections 3.3 and 3.4, respectively. Finally, we summarize our results in section 4.

2 Field equations and numerical setup

The nonrelativistic dynamics of ultralight dark matter can be described by the Schroedinger equation coupled to gravity through Poisson’s equation [1–4, 91]. When incorporating both minimal and nonminimal couplings to gravity, the Schroedinger-Poisson equations for scalar

²Nonminimal couplings to gravity could arise from quantum corrections and are essential for the renormalization of field theories in curved spacetime [68–72]. Their phenomenological implications have been studied in various contexts, such as dark matter [67, 73–76], inflation [77–84], and modified gravity [85–90].

dark matter are [8]

$$i\partial_t\psi = -\frac{\nabla^2}{2m}\psi + m\Phi\psi + \frac{\xi}{2mM_P^2}\rho_\xi\psi, \quad (2.1)$$

$$\nabla^2\Phi = \frac{1}{2M_P^2}\rho_\xi, \quad (2.2)$$

where ψ is a nonrelativistic classical field that varies slowly in time, m is the field mass, Φ is the gravitational potential, ξ characterizes NGIs, and ρ_ξ is the mass density defined as $\rho_\xi \equiv \rho + (\xi/m^2)\nabla^2\rho$ with $\rho \equiv m|\psi|^2$. The natural units $c = \hbar = 1$ are adopted. In this work, we focus on time scales short compared with the Hubble time, thus neglecting the expansion of the universe.

Unlike the usual equations used in the literature [1–4], Poisson’s equation here is sourced by ρ_ξ rather than the rest mass density ρ due to nonminimal gravitational effects. The NGI term in (2.1) has two components: one resembles the self-interaction from a quartic scalar dark matter coupling, and the other depends on the density gradient. As shown in [8], the gradient-dependent part imposes an upper limit on the density hence mass of dark matter solitons, independent of the sign of ξ . We will discuss it in more details in section 3.2.

The equations (2.1) and (2.2) can be simplified by introducing the dimensionless quantities (denoted with tilde):

$$t \rightarrow \frac{\tilde{t}}{v^2m}, \quad \mathbf{x} \rightarrow \frac{\tilde{\mathbf{x}}}{vm}, \quad \Phi \rightarrow v^2\tilde{\Phi}, \quad \psi_i \rightarrow v^2\sqrt{m}F\tilde{\psi}_i, \quad \xi \rightarrow \frac{\tilde{\xi}}{v^2}, \quad (2.3)$$

where v is an arbitrary positive constant and F is a chosen mass scale, which we set $F = \sqrt{2}M_P$. As a result, equations (2.1) and (2.2) transform to

$$i\partial_{\tilde{t}}\tilde{\psi} = -\frac{\tilde{\nabla}^2}{2}\tilde{\psi} + \tilde{\Phi}\tilde{\psi} + \tilde{\xi}\tilde{\rho}_\xi\tilde{\psi}, \quad (2.4)$$

$$\tilde{\nabla}^2\tilde{\Phi} = \tilde{\rho}_\xi, \quad (2.5)$$

where the mass density $\tilde{\rho}_\xi = \tilde{\rho} + \tilde{\xi}\tilde{\nabla}^2\tilde{\rho}$ and the particle number density $\tilde{\rho} = |\tilde{\psi}|^2$. These equations are independent of v , implying a scaling symmetry that allows us to set $|\tilde{\xi}| = 1$. However, to manage numerical challenges associated with small-scale structures and long-term evolution, we will retain flexibility in choosing different values for $\tilde{\xi}$.

To simulate the Schroedinger-Poisson equations (2.4) and (2.5), we employ a fourth-order pseudospectral method as described in [92–94], treating the NGI term in the Schroedinger equation as an additional part of the potential. Initial conditions are set in momentum space with a delta-like distribution $|\tilde{\psi}_{\tilde{\mathbf{p}}}|^2 \propto \delta(|\tilde{\mathbf{p}}| - v_0/v)$ and a random phase. Here, $v_0 \ll 1$ is a reference velocity for the nonrelativistic system, but its exact value is unimportant due to the freedom in choosing v . For simplicity, we set $v = v_0$. Alternative initial conditions, such as a Gaussian distribution $|\tilde{\psi}_{\tilde{\mathbf{p}}}|^2 \propto e^{-\tilde{\mathbf{p}}^2}$ or a step-like distribution $|\tilde{\psi}_{\tilde{\mathbf{p}}}|^2 \propto \theta(v_0/v - |\tilde{\mathbf{p}}|)$, may also be used. However, the formation of dark matter halos and solitons is largely insensitive to the initial distribution [10]. To study isolated halos, we run simulations in a box with size $\tilde{L} > 2\pi/\tilde{k}_J$, where $\tilde{k}_J = (4\tilde{\rho})^{1/4}$ is the Jeans scale, with a bar over variables indicating their spatial mean value. The box size is set to $\tilde{L} = 18$ and the total number of particles to $\tilde{N} = 1005.3$.

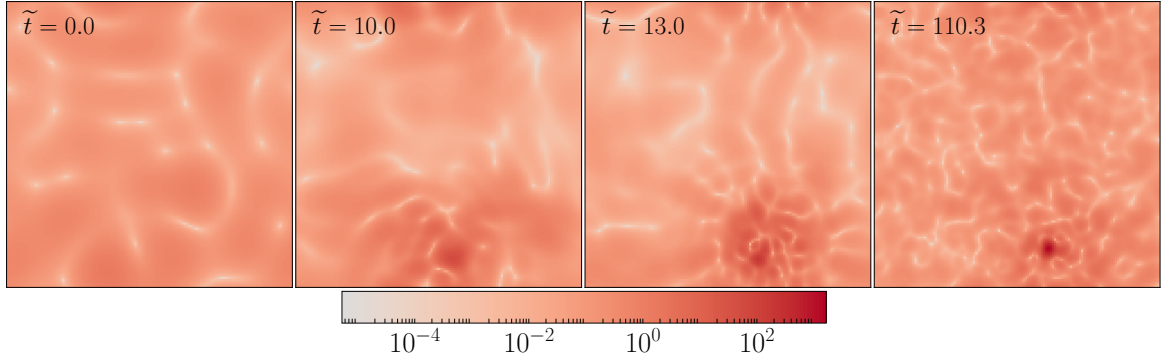


Figure 1. Evolution of dark matter without nonminimal gravitational effects, illustrated by slices of the particle number density $\tilde{\rho}$ at different times. These slices show the density on a plane passing through the peak density location. We see that a dense dark matter halo forms gradually over time, with a soliton clearly emerging at the halo's center by $\tilde{t} \approx 110$.

3 Formation and collapse of solitons in dark matter halos

In this section, we examine how solitons form, grow and collapse in dark matter halos influenced by NGIs. We begin by reviewing the soliton formation process in the absence of NGIs (i.e., $\tilde{\xi} = 0$) in section 3.1. Next, we outline some key properties of solitons in section 3.2. We then analyze the impact of NGIs with positive and negative coupling constants $\tilde{\xi}$ in sections 3.3 and 3.4, respectively.

3.1 Condensation of self-gravitating solitons

For self-gravitating dark matter without NGIs, studies have demonstrated that gravity induces the formation of solitons at the centers of dark matter halos. The condensation timescale for dark matter particles within a halo of size R_h is given by [10]

$$t_{\text{gr}} = \frac{16\sqrt{2}b}{3\pi} \frac{M_{\text{P}}^4 m v_0^6}{n^2 \Lambda} , \quad (3.1)$$

where b is an $\mathcal{O}(1)$ coefficient determined by simulations, v_0 is the characteristic velocity, n is the typical number density, and $\Lambda = \log(m v_0 R_h)$ is the Coulomb logarithm. Once formed, solitons continue to grow by accreting mass from the surrounding gas of particles at a rate $M_s \propto t^{1/2}$ [10]. As the soliton grows sufficiently large, it begins to heat the surrounding halo and makes the whole system reach virial equilibrium after a few condensation times t_{gr} [13]. The mass growth of solitons is then slowed down to a rate $M_s \propto t^{1/8}$ [13, 17] or $t^{1/4}$ [49]. These findings present conflicting results; however, recent work suggests that the soliton mass evolves not as a simple power law over time, potentially encompassing both of these behaviors [50]. This paper does not delve into resolving this debate.

For completeness, we simulate dark matter without NGIs and present the structure formation in figure 1. We observe the gradual formation of a dense dark matter halo from $\tilde{t} = 0$ to $\tilde{t} = 10$. By $\tilde{t} \approx 110$, a distinct dense object, with a density profile closely resembling a soliton solution, becomes evident at the halo's center, in agreement with the soliton condensation timescale given by (3.1).

3.2 Nonminimally gravitating solitons

The natural emergence of solitons in dark matter halos can be attributed to their status as ground states of the Schroedinger-Poisson equations at fixed particle number [6, 95, 96], making them energetically favorable in a thermal bath of nonrelativistic particles. In this subsection, we provide a concise overview of key properties of solitons in the presence of NGIs, following [8].

Generally speaking, scalar solitons take the form $\tilde{\psi}(\tilde{t}, \tilde{x}) = \tilde{f}(\tilde{r})e^{i\tilde{\mu}\tilde{t}}$, where $\tilde{\mu}$ is the chemical potential and \tilde{f} represents a spherically symmetric profile. The field equations (2.4) and (2.5) then translate into radial profile equations for \tilde{f} and $\tilde{\Phi}$:

$$-\frac{1}{2}\tilde{\nabla}^2\tilde{f} + (\tilde{\Phi} + \tilde{\mu})\tilde{f} + \tilde{\xi}\tilde{f}^3 + \tilde{\xi}^2\tilde{f}\tilde{\nabla}^2\tilde{f}^2 = 0, \quad (3.2)$$

and $\tilde{\nabla}^2\tilde{\Phi} = \tilde{f}^2 + \tilde{\xi}\tilde{\nabla}^2\tilde{f}^2$. Soliton solutions can then be found by taking the boundary conditions $\partial_{\tilde{r}}\tilde{f}|_{\tilde{r}=0} = \partial_{\tilde{r}}\tilde{\Phi}|_{\tilde{r}=0} = 0$ and $\partial_{\tilde{r}}\tilde{f}|_{\tilde{r}\rightarrow\infty} = 0$. Some examples are shown as solid curves in figures 3 and 6, obtained using the Mathematica package DMSolitonFinder developed by one of us [8].

The term $\tilde{\xi}\tilde{f}^3$ in (3.2) plays a similar role to a quartic self-coupling of the progenitor Lorentz scalar field. A positive $\tilde{\xi}$ tends to compactify solitons, requiring more matter to balance the induced repulsive force. A negative $\tilde{\xi}$ destabilizes solitons as their mass increases, reaching a critical density where the induced attractive force competes with gravity. At the critical densities,

$$\tilde{\rho}^{\max} = 0.0458|\tilde{\xi}|^{-2} \quad \text{and} \quad \tilde{\rho}_{\xi}^{\max} = 0.0884|\tilde{\xi}|^{-2} \quad (\text{for } \tilde{\xi} < 0), \quad (3.3)$$

solitons collapse until the relativistic theory is warranted to depict the full story.

The impact of the gradient-dependent part of NGIs in equation (3.2), $\tilde{\xi}^2\tilde{f}\tilde{\nabla}^2\tilde{f}^2$, is more complex. A positive $\tilde{\xi}$ makes the mass density $\tilde{\rho}_{\xi}$ less than the particle number density $\tilde{\rho}$ and thus induces a repulsive force within soliton cores, with causing opposite effects in the outer regions. It also imposes an upper limit on central soliton amplitudes, $\tilde{f}_0^{\max} = |2\tilde{\xi}|^{-1}$. This corresponds to the maximum densities

$$\tilde{\rho}^{\max} = 0.250\tilde{\xi}^{-2} \quad \text{and} \quad \tilde{\rho}_{\xi}^{\max} = 0.0746\tilde{\xi}^{-2} \quad (\text{for } \tilde{\xi} > 0). \quad (3.4)$$

In such critical solitons, the repulsive force is sufficiently strong that the core may exhibit negative density $\tilde{\rho}_{\xi}$, as we will see in next subsection. Similar amplitude and density bounds exist for negative $\tilde{\xi}$, which nevertheless remain on the unstable branch of solitons and thus do not have significant impact.

3.3 Dark matter with positive nonminimal couplings

To explore the formation of dark matter halos and solitons under the influence of NGIs in an efficient way, we need to determine an appropriate magnitude for $\tilde{\xi}$. A useful quantity for assessing the importance of NGIs is the Jeans scale, which govern the scales of linearized perturbations that experience rapid growth. For $\tilde{\xi}\sqrt{\tilde{\rho}} < 1$, the Jeans scale is approximately given by $\tilde{k}_J \approx (4\tilde{\rho})^{1/4}[1 + \tilde{\xi}\sqrt{\tilde{\rho}}]$ [67], indicating that NGIs may only be relevant if $\tilde{\xi}\sqrt{\tilde{\rho}} \gtrsim 1$. However, nonlinear analysis of solitons suggests that NGIs start to significantly affect dynamics around $\tilde{\xi}\sqrt{\tilde{\rho}} \sim 0.3$, as indicated by (3.3) and (3.4). Therefore, we adopt $|\tilde{\xi}| \sim \mathcal{O}(0.01)$ for our simulations. At these values of $|\tilde{\xi}|$, the initial evolution of dark matter resembles that

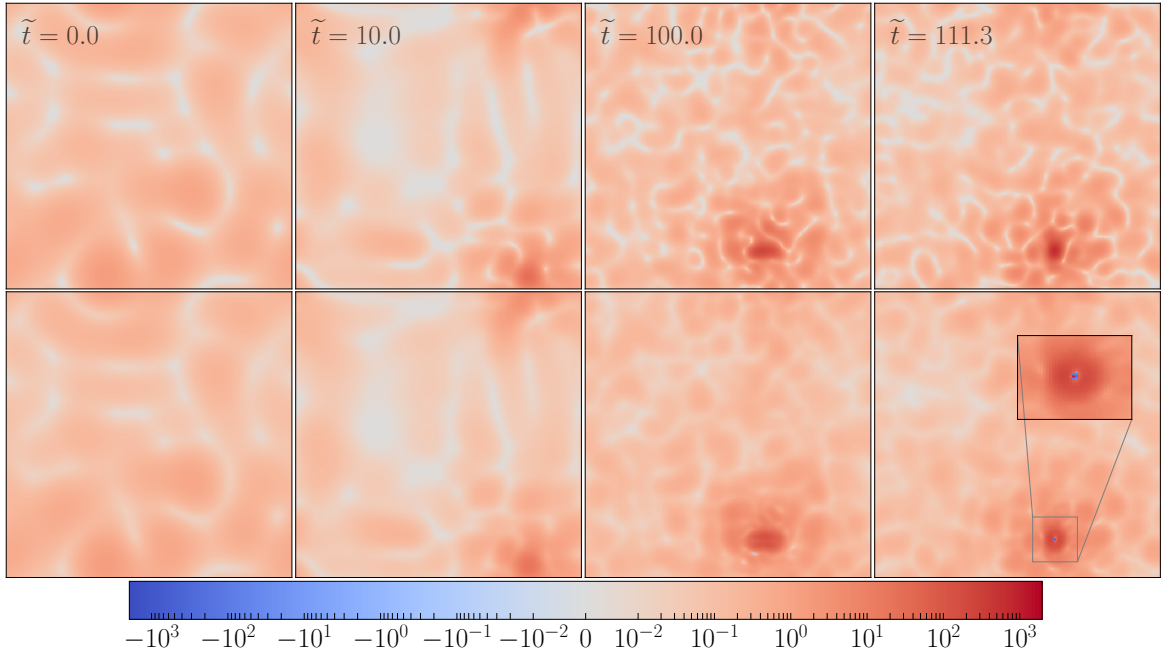


Figure 2. Evolution of dark matter with $\tilde{\xi} = 0.02$, illustrated by slices of the number density $\tilde{\rho}$ (in upper panels) and the mass density $\tilde{\rho}_\xi$ (in lower panels) at different times. By $\tilde{t} = 100$, a soliton has formed at the halo's center. As the soliton grows, the mass density $\tilde{\rho}_\xi$ in its inner core becomes negative when the soliton collapses at $\tilde{t} \approx 111.3$.

without NGIs and the condensation time scale (3.1) will not be significantly affected, but the impact of NGIs becomes pronounced at later times $\tilde{t} \sim \mathcal{O}(10)$ as inhomogeneities develop.

In figure 2, we show the evolution of dark matter densities $\tilde{\rho}$ (in upper panels) and $\tilde{\rho}_\xi$ (in lower panels) with $\tilde{\xi} = 0.02$. At early times $\tilde{t} \lesssim 10$, a dark matter halo gradually forms, during which the distributions of $\tilde{\rho}$ and $\tilde{\rho}_\xi$ look quite similar. Their difference, $\tilde{\rho}_\xi - \tilde{\rho} = \tilde{\xi} \nabla^2 \tilde{\rho}$, remains suppressed since inhomogeneities are not sufficiently developed.

By $\tilde{t} = 100$, the center of the halo becomes very dense, indicating the presence of a soliton. This is confirmed by comparing density profiles of the halo and the soliton solution with the same particle number density $\tilde{\rho}$ at the center. Figure 3 shows the density profiles of the halo and the corresponding soliton solution at various times (dots and solid lines, respectively). As matter accretes, the $\tilde{\rho}_\xi$ profile at small radii becomes increasingly sensitive to the selection of the halo's center. The inset of the right plot displays 27 profiles extracted at $\tilde{t} = 110$ by taking slightly different locations around the maximum $\tilde{\rho}$ as the halo's center (gray lines). They differ at $\tilde{r} \lesssim 2|\tilde{\xi}|^{1/2}$ but converge at larger radii. To mitigate this uncertainty, we average these 27 profiles to obtain numerical data points solely for $\tilde{\rho}_\xi$ with $\tilde{\xi} = 0.02$. Both $\tilde{\rho}$ and $\tilde{\rho}_\xi$ profiles show that the halo and soliton solution coincide well at $\tilde{r} \lesssim 5|\tilde{\xi}|^{1/2}$. In contrast, solitons with $\tilde{\xi} = 0$ (dashed lines) poorly fit the numerical data.

The soliton keeps growing after formation and is expected to collapse when its densities reach the critical values (3.4). This prediction is verified through multiple simulations with various values of $\tilde{\xi}$. In figure 4, the evolution of the maximum density $\tilde{\rho}_\xi^{\max}$ is represented by solid lines, while dashed lines indicate the corresponding critical densities. At collapse, the soliton radius, defined as the radius where the particle number density $\tilde{\rho}$ drops to half of its

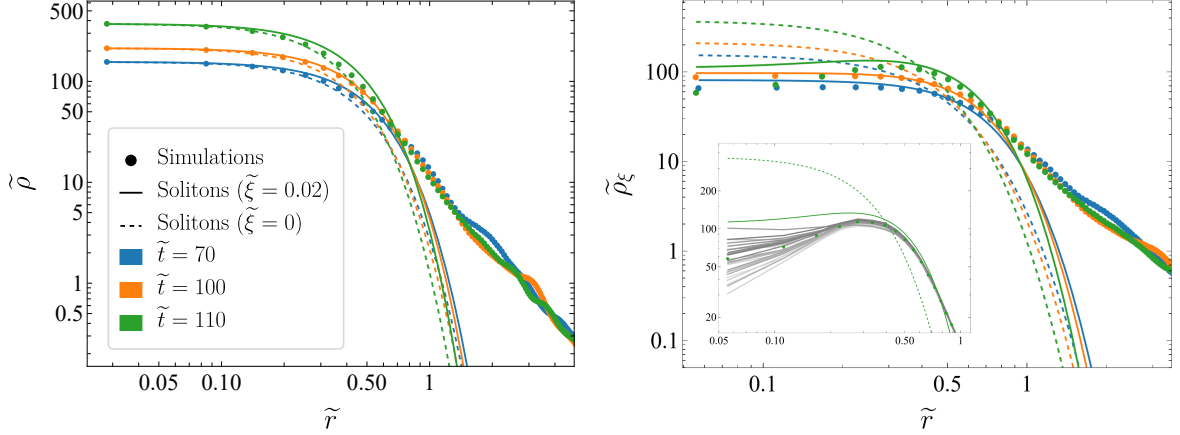


Figure 3. Density profiles of the halo at different times. The data points are taken from simulations with $\xi = 0.02$, and are well fitted by the soliton solution with an identical number density $\tilde{\rho}$ at the center (solid lines). Soliton profiles without NGIs are also shown for comparison (dashed lines). For the numerical data points of $\tilde{\rho}_\xi$, we average 27 profiles (gray lines in the inset, obtained at $\tilde{t} = 110$ for illustration) extracted by considering slightly different locations as the halo’s center to mitigate numerical errors.

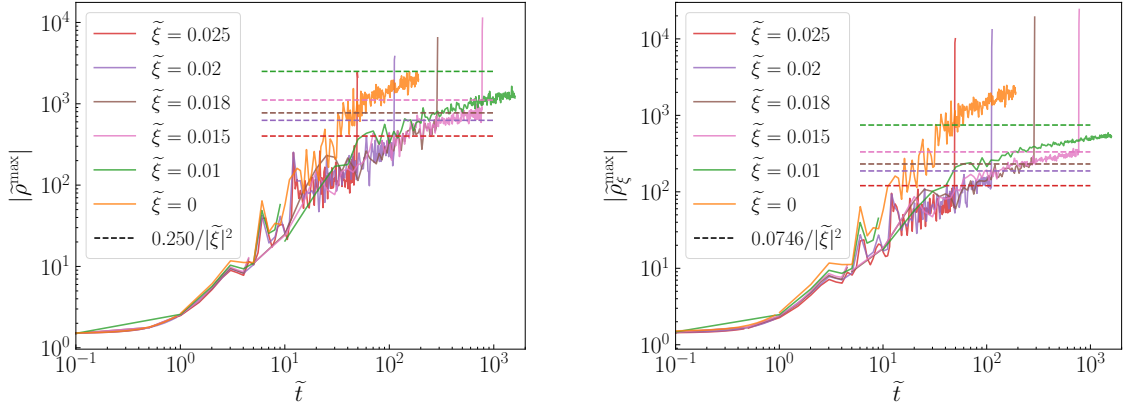


Figure 4. Evolution of the maximum number density $\tilde{\rho}^{\max}$ (left) and the maximum mass density $\tilde{\rho}_\xi^{\max}$ (right) for various positive NGI couplings. Dashed lines indicate the maximum densities predicted by (3.4), beyond which solitons are expected to collapse.

central value, is given by

$$R_s = 1.36 \times 10^8 \text{ km} \left(\frac{\xi}{10} \right) \left(\frac{10^{-18} \text{ eV}}{m} \right). \quad (3.5)$$

Due to the gradient-independent part of NGIs, one may expect a regime where gravity is counterbalanced by repulsive NGIs, with negligible quantum pressure, allowing solitons to be well described by the Thomas-Fermi approximation [17]. However, this regime lies beyond the critical densities (3.4) and cannot be achieved dynamically via gravitational accretion.

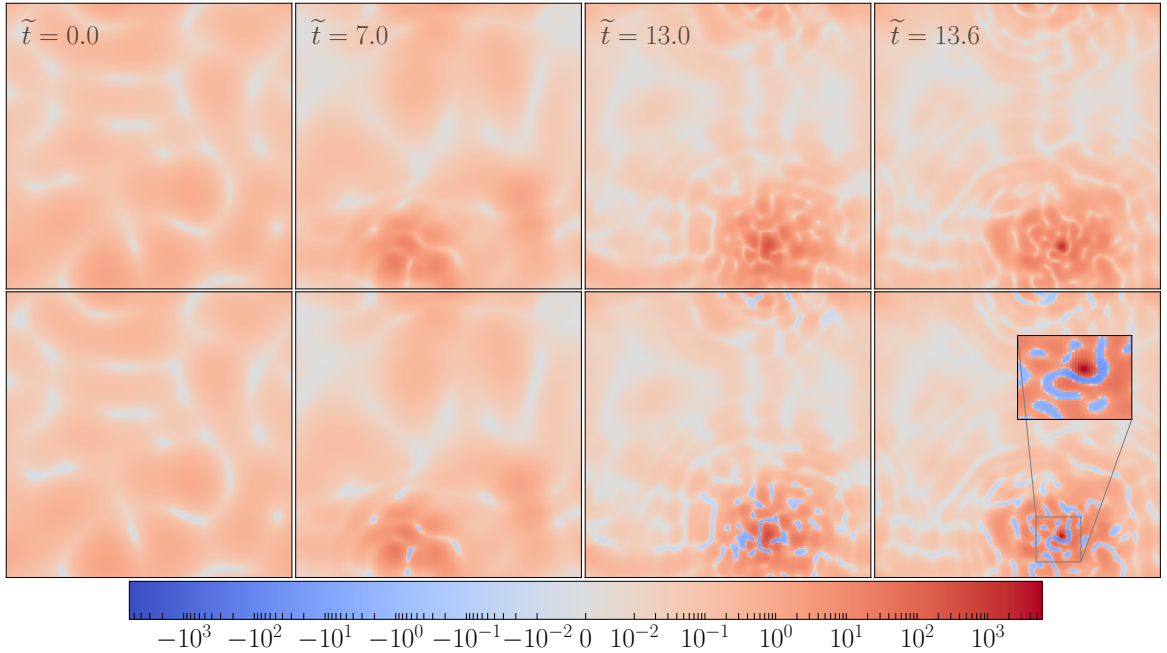


Figure 5. Evolution of dark matter with $\tilde{\xi} = -0.008$, illustrated by slices of the number density $\tilde{\rho}$ (in upper panels) and the mass density $\tilde{\rho}_\xi$ (in lower panels) at different times. By $\tilde{t} = 13$, a soliton has formed at the center of the halo, surrounded by multiple subhalos. These subhalos could contain more mass than particle numbers, with regions showing negative mass density $\tilde{\rho}_\xi$ in the voids between them.

3.4 Dark matter with negative nonminimal couplings

In this subsection, we examine the evolution of dark matter with negative $\tilde{\xi}$. Figure 5 illustrates the evolution of dark matter densities $\tilde{\rho}$ (upper panels) and $\tilde{\rho}_\xi$ (lower panels) with $\tilde{\xi} = -0.008$. Similar to the case with positive couplings, we observe that the difference between $\tilde{\rho}$ and $\tilde{\rho}_\xi$ is small during the initial stages of evolution. By $\tilde{t} = 13$, a cluster of dark matter halos has formed, containing a central soliton surrounded by many subhalos. The profiles of the soliton are depicted in figure 6. The subhalos typically contain higher mass than particle numbers, with regions exhibiting negative mass density $\tilde{\rho}_\xi$ in the voids between them.

The evolution of maximum densities are shown in figure 5. The soliton continues to grow after formation and eventually collapses when its maximum densities predicted by (3.3) (indicated by the dashed lines), as expected. Above the critical values, solitons are no longer energetically favored states and become unstable to perturbations. At collapse, the radius of the soliton, where the particle number density drops to half of its central value, is given by

$$R_s = 4.32 \times 10^8 \text{ km} \left(\frac{|\xi|}{10} \right) \left(\frac{10^{-18} \text{ eV}}{m} \right) . \quad (3.6)$$

As mentioned in section 3.2, there exist additional upper limits on soliton densities due to the gradient-dependent part of NGIs. However, these densities correspond to the unstable branch and are not accessible in our simulations.

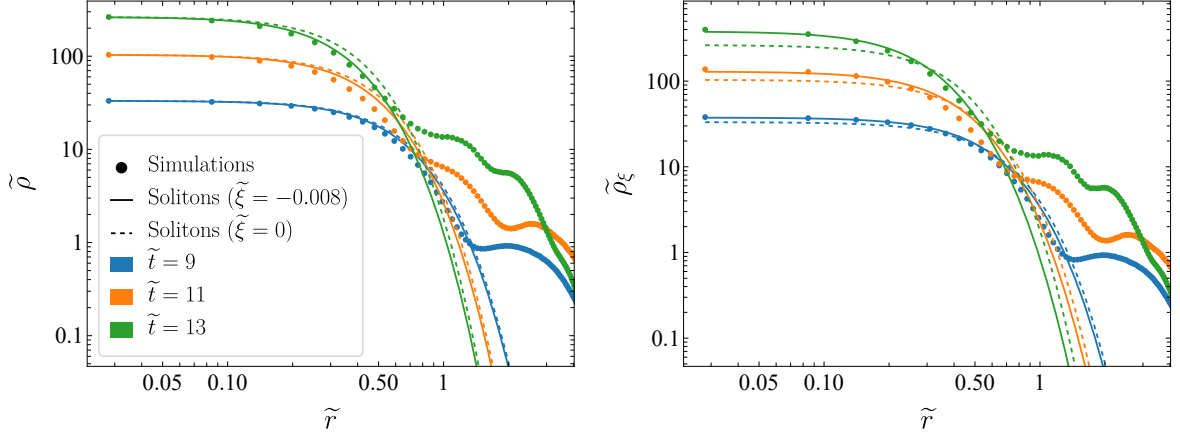


Figure 6. Density profiles of the halo at different times. The data points are taken from simulations with $\tilde{\xi} = -0.008$, and are well fitted by the soliton solution with an identical number density $\tilde{\rho}$ at the center (solid lines). Soliton profiles without NGIs are also shown for comparison (dashed lines).

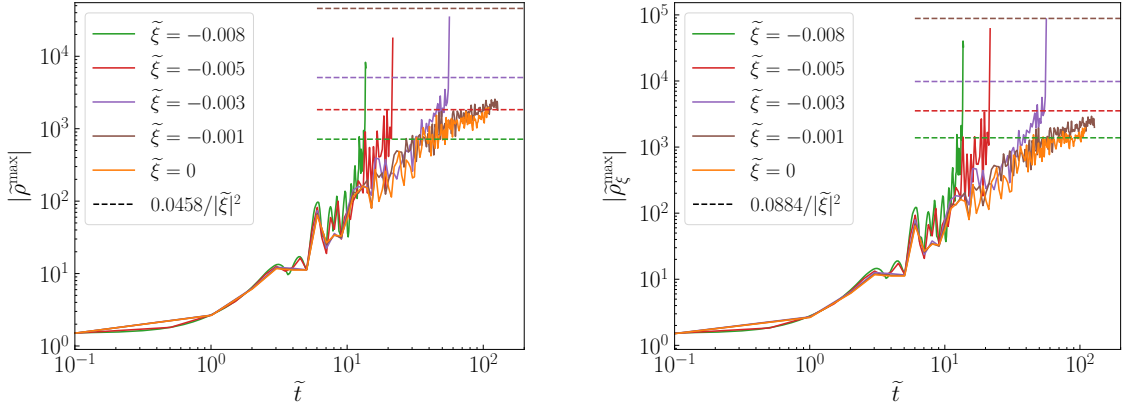


Figure 7. Evolution of the maximum number density $|\tilde{\rho}^{\max}|$ (left) and the maximum mass density $|\tilde{\rho}_\xi^{\max}|$ (right) for various negative NGI couplings. Dashed lines indicate the maximum densities predicted by (3.3), beyond which solitons are expected to collapse.

4 Conclusions

In this work, we study the formation, growth, and collapse of solitons within halos of non-minimally gravitating dark matter, characterized by both gradient-independent and gradient-dependent self-interactions in the nonrelativistic regime. This latter component, despite being overlooked in parameterizations for self-interacting ultralight dark matter, could have important implications for the phenomenology of dark matter and its solitons. We investigate the effects by numerically evolving the nonlinear Schrödinger-Poisson equations (2.4) and (2.5). Although our simulations are not cosmological, our findings are relevant in cosmological models possessing appropriate environments.

In figures 4 and 7, we demonstrate that for both positive and negative coupling constants $\tilde{\xi}$, solitons collapse when their densities exceed certain critical values given by equations (3.3) and (3.4). The mass of collapsing solitons is at the level of $\sim 40M_P^2/(m|\xi|^{1/2})$ [8]. Once the

critical densities are reached, the dark matter clump rapidly grows, necessitating relativistic simulations for further evolution. In contrast, solitons with solely gradient-independent self-interactions will collapse only for negative couplings, i.e., attractive self-interactions [17, 97, 98]. Collapsing solitons undergo a series of bursts and could be potentially detected if dark matter is coupled to regular matter [65].

Another novel aspect of nonminimally gravitating dark matter is the inclusion of a gradient-dependent source in the Poisson's equation (2.2), alongside the rest mass density. This leads us to consider a modified mass density ρ_ξ that maintains the familiar Newton's law. Our numerical results suggest that solitons with positive couplings could feature an inner core with negative mass density via dynamical matter accretion, as shown in figure 2. For negative couplings, subhalos surrounding the central soliton could have more mass than particle numbers with voids of negative mass density in between, see figure 5. These characteristics could have novel implications for gravitational lensing [99], dynamic heating of stars [100], and axion minivoids [101], warranting further investigation.

We also simulate systems with stronger nonminimal couplings of the order $\tilde{\xi}\sqrt{\tilde{\rho}} \sim \mathcal{O}(0.1)$. In these cases, structure formation is significantly enhanced and density spikes rapidly develop beyond our numerical resolutions. The fast formation can be understood by noting that linearized density perturbations could grow on both large and small scales if the nonminimal coupling is strong enough that $\tilde{\xi}\sqrt{\tilde{\rho}} \sim 1$ [67]. We verify this novel pattern by limiting the simulation box to below the usual Jeans scale, i.e., $\tilde{L} < 2\pi/\tilde{k}_J$. We observe the development of mini structures, though our simulations quickly break down due to amplified noise.

In conclusion, our study reveals novel insights into the formation and growth of dark matter halos and solitons influenced by nonminimal gravitational effects. This research opens up new avenues for probing ultralight dark matter and modified gravity through cosmological and astrophysical observations.

Acknowledgments

We would like to thank Xiaolong Du and Luca Visinelli for helpful comments. We would especially like to thank Zhipan Li for his assistance in setting up the clusters. JC acknowledges the support from the Fundamental Research Funds for the Central Universities (SWU-KR22012) and the Chongqing Natural Science Foundation General Project (2023NSCQ-MSX1929). HYZ is supported in part by the National Natural Science Foundation of China (NSFC) through grant No. 12350610240. This research was also facilitated by the computational resources in the School of Physical Science and Technology at Southwest University.

References

- [1] L. Hui, *Wave Dark Matter*, *Ann. Rev. Astron. Astrophys.* **59** (2021) 247 [[2101.11735](https://arxiv.org/abs/2101.11735)].
- [2] E. G. M. Ferreira, *Ultra-light dark matter*, *Astron. Astrophys. Rev.* **29** (2021) 7 [[2005.03254](https://arxiv.org/abs/2005.03254)].
- [3] T. Matos, L. A. Ureña López and J.-W. Lee, *Short review of the main achievements of the scalar field, fuzzy, ultralight, wave, BEC dark matter model*, *Front. Astron. Space Sci.* **11** (2024) 1347518 [[2312.00254](https://arxiv.org/abs/2312.00254)].
- [4] C. A. J. O'Hare, *Cosmology of axion dark matter*, *PoS COSMICWISPer* (2024) 040 [[2403.17697](https://arxiv.org/abs/2403.17697)].

[5] W. Hu, R. Barkana and A. Gruzinov, *Cold and fuzzy dark matter*, *Phys. Rev. Lett.* **85** (2000) 1158 [[astro-ph/0003365](#)].

[6] L. Hui, J. P. Ostriker, S. Tremaine and E. Witten, *Ultralight scalars as cosmological dark matter*, *Phys. Rev. D* **95** (2017) 043541 [[1610.08297](#)].

[7] A. H. Guth, M. P. Hertzberg and C. Prescod-Weinstein, *Do Dark Matter Axions Form a Condensate with Long-Range Correlation?*, *Phys. Rev. D* **92** (2015) 103513 [[1412.5930](#)].

[8] H.-Y. Zhang, *Unified view of scalar and vector dark matter solitons*, [2406.05031](#).

[9] H.-Y. Schive, T. Chiueh and T. Broadhurst, *Cosmic Structure as the Quantum Interference of a Coherent Dark Wave*, *Nature Phys.* **10** (2014) 496 [[1406.6586](#)].

[10] D. Levkov, A. Panin and I. Tkachev, *Gravitational Bose-Einstein condensation in the kinetic regime*, *Phys. Rev. Lett.* **121** (2018) 151301 [[1804.05857](#)].

[11] J. Veltmaat, J. C. Niemeyer and B. Schwabe, *Formation and structure of ultralight bosonic dark matter halos*, *Phys. Rev. D* **98** (2018) 043509 [[1804.09647](#)].

[12] P. Mocz et al., *First star-forming structures in fuzzy cosmic filaments*, *Phys. Rev. Lett.* **123** (2019) 141301 [[1910.01653](#)].

[13] B. Eggemeier and J. C. Niemeyer, *Formation and mass growth of axion stars in axion miniclusters*, *Phys. Rev. D* **100** (2019) 063528 [[1906.01348](#)].

[14] S. May and V. Springel, *Structure formation in large-volume cosmological simulations of fuzzy dark matter: impact of the non-linear dynamics*, *Mon. Not. Roy. Astron. Soc.* **506** (2021) 2603 [[2101.01828](#)].

[15] D. Ellis, D. J. E. Marsh, B. Eggemeier, J. Niemeyer, J. Redondo and K. Dolag, *Structure of axion miniclusters*, *Phys. Rev. D* **106** (2022) 103514 [[2204.13187](#)].

[16] M. Gorgetto, E. Hardy, J. March-Russell, N. Song and S. M. West, *Dark photon stars: formation and role as dark matter substructure*, *JCAP* **08** (2022) 018 [[2203.10100](#)].

[17] J. Chen, X. Du, E. W. Lentz, D. J. E. Marsh and J. C. Niemeyer, *New insights into the formation and growth of boson stars in dark matter halos*, *Phys. Rev. D* **104** (2021) 083022.

[18] M. A. Amin, M. Jain, R. Karur and P. Mocz, *Small-scale structure in vector dark matter*, *JCAP* **08** (2022) 014 [[2203.11935](#)].

[19] J. Chen, X. Du, M. Zhou, A. Benson and D. J. E. Marsh, *Gravitational bose-einstein condensation of vector or hidden photon dark matter*, *Phys. Rev. D* **108** (2023) 083021.

[20] M. Jain, M. A. Amin, J. Thomas and W. Wanichwecharungruang, *Kinetic relaxation and Bose-star formation in multicomponent dark matter*, *Phys. Rev. D* **108** (2023) 043535 [[2304.01985](#)].

[21] M. Jain, W. Wanichwecharungruang and J. Thomas, *Kinetic relaxation and nucleation of Bose stars in self-interacting wave dark matter*, *Phys. Rev. D* **109** (2024) 016002 [[2310.00058](#)].

[22] M. Milosavljevic and D. Merritt, *The Final parsec problem*, *AIP Conf. Proc.* **686** (2003) 201 [[astro-ph/0212270](#)].

[23] H. Koo, D. Bak, I. Park, S. E. Hong and J.-W. Lee, *Final parsec problem of black hole mergers and ultralight dark matter*, [2311.03412](#).

[24] B. C. Bromley, P. Sandick and B. Shams Es Haghi, *Supermassive Black Hole Binaries in Ultralight Dark Matter*, [2311.18013](#).

[25] G. Alonso-Álvarez, J. M. Cline and C. Dewar, *Self-Interacting Dark Matter Solves the Final Parsec Problem of Supermassive Black Hole Mergers*, *Phys. Rev. Lett.* **133** (2024) 021401 [[2401.14450](#)].

[26] B. Kocsis and A. Sesana, *Gas driven massive black hole binaries: signatures in the nHz gravitational wave background*, *Mon. Not. Roy. Astron. Soc.* **411** (2011) 1467 [[1002.0584](#)].

[27] F. G. Goicovic, A. Sesana, J. Cuadra and F. Stasyszyn, *Infalling clouds on to supermassive black hole binaries – II. Binary evolution and the final parsec problem*, *Mon. Not. Roy. Astron. Soc.* **472** (2017) 514 [[1602.01966](#)].

[28] F. G. Goicovic, C. Maureira-Fredes, A. Sesana, P. Amaro-Seoane and J. Cuadra, *Accretion of clumpy cold gas onto massive black hole binaries: a possible fast route to binary coalescence*, *Mon. Not. Roy. Astron. Soc.* **479** (2018) 3438 [[1801.04937](#)].

[29] F. M. Khan, K. Holley-Bockelmann, P. Berczik and A. Just, *Supermassive Black Hole Binary Evolution in Axisymmetric Galaxies: The final parsec problem is not a problem*, *Astrophys. J.* **773** (2013) 100 [[1302.1871](#)].

[30] E. Vasiliev, F. Antonini and D. Merritt, *The final-parsec problem in nonspherical galaxies revisited*, *Astrophys. J.* **785** (2014) 163 [[1311.1167](#)].

[31] H.-Y. Schive, M.-H. Liao, T.-P. Woo, S.-K. Wong, T. Chiueh, T. Broadhurst et al., *Understanding the Core-Halo Relation of Quantum Wave Dark Matter from 3D Simulations*, *Phys. Rev. Lett.* **113** (2014) 261302 [[1407.7762](#)].

[32] D. J. E. Marsh and A.-R. Pop, *Axion dark matter, solitons and the cusp–core problem*, *Mon. Not. Roy. Astron. Soc.* **451** (2015) 2479 [[1502.03456](#)].

[33] S.-R. Chen, H.-Y. Schive and T. Chiueh, *Jeans Analysis for Dwarf Spheroidal Galaxies in Wave Dark Matter*, *Mon. Not. Roy. Astron. Soc.* **468** (2017) 1338 [[1606.09030](#)].

[34] A. X. González-Morales, D. J. E. Marsh, J. Peñarrubia and L. A. Ureña López, *Unbiased constraints on ultralight axion mass from dwarf spheroidal galaxies*, *Mon. Not. Roy. Astron. Soc.* **472** (2017) 1346 [[1609.05856](#)].

[35] T. Broadhurst, I. de Martino, H. N. Luu, G. F. Smoot and S. H. H. Tye, *Ghostly Galaxies as Solitons of Bose-Einstein Dark Matter*, *Phys. Rev. D* **101** (2020) 083012 [[1902.10488](#)].

[36] N. Bar, D. Blas, K. Blum and S. Sibiryakov, *Galactic rotation curves versus ultralight dark matter: Implications of the soliton-host halo relation*, *Phys. Rev. D* **98** (2018) 083027 [[1805.00122](#)].

[37] I. De Martino, T. Broadhurst, S. H. H. Tye, T. Chiueh and H.-Y. Schive, *Dynamical Evidence of a Solitonic Core of $10^9 M_\odot$ in the Milky Way*, *Phys. Dark Univ.* **28** (2020) 100503 [[1807.08153](#)].

[38] A. Pozo, T. Broadhurst, G. F. Smoot and T. Chiueh, *Dwarf Galaxies United by Dark Bosons*, [2302.00181](#).

[39] PARTICLE DATA GROUP collaboration, *Review of Particle Physics*, *PTEP* **2022** (2022) 083C01.

[40] S. Chakrabarti, B. Dave, K. Dutta and G. Goswami, *Constraints on the mass and self-coupling of ultra-light scalar field dark matter using observational limits on galactic central mass*, *JCAP* **09** (2022) 074 [[2202.11081](#)].

[41] B. Dave and G. Goswami, *ULDM self-interactions, tidal effects and tunnelling out of satellite galaxies*, *JCAP* **02** (2024) 044 [[2310.19664](#)].

[42] B. Dave and G. Goswami, *Self-interactions of ULDM to the rescue?*, *JCAP* **07** (2023) 015 [[2304.04463](#)].

[43] M. P. Hertzberg and E. D. Schiappacasse, *Dark Matter Axion Clump Resonance of Photons*, *JCAP* **11** (2018) 004 [[1805.00430](#)].

[44] M. P. Hertzberg, Y. Li and E. D. Schiappacasse, *Merger of Dark Matter Axion Clumps and Resonant Photon Emission*, *JCAP* **07** (2020) 067 [[2005.02405](#)].

[45] M. A. Amin and Z.-G. Mou, *Electromagnetic Bursts from Mergers of Oscillons in Axion-like Fields*, *JCAP* **02** (2020) 024 [[2009.11337](#)].

[46] M. A. Amin, A. J. Long, Z.-G. Mou and P. Saffin, *Dipole radiation and beyond from axion stars in electromagnetic fields*, *JHEP* **06** (2021) 182 [[2103.12082](#)].

[47] M. A. Amin, A. J. Long and E. D. Schiappacasse, *Photons from dark photon solitons via parametric resonance*, *JCAP* **05** (2023) 015 [[2301.11470](#)].

[48] D. Levkov, E. Nugaev and A. Popescu, *The fate of small classically stable Q-balls*, *JHEP* **12** (2017) 131 [[1711.05279](#)].

[49] J. H.-H. Chan, S. Sibiryakov and W. Xue, *Condensation and evaporation of boson stars*, *JHEP* **01** (2024) 071 [[2207.04057](#)].

[50] A. S. Dmitriev, D. G. Levkov, A. G. Panin and I. I. Tkachev, *Self-Similar Growth of Bose Stars*, *Phys. Rev. Lett.* **132** (2024) 091001 [[2305.01005](#)].

[51] J. Veltmaat, B. Schwabe and J. C. Niemeyer, *Baryon-driven growth of solitonic cores in fuzzy dark matter halos*, *Phys. Rev. D* **101** (2020) 083518 [[1911.09614](#)].

[52] J. H. Chan, H.-Y. Schive, T.-P. Woo and T. Chiueh, *How do stars affect ψ dm haloes?*, *Monthly Notices of the Royal Astronomical Society* **478** (2018) 2686.

[53] J. Bovy and S. Tremaine, *On the local dark matter density*, *Astrophys. J.* **756** (2012) 89 [[1205.4033](#)].

[54] M. Pato, F. Iocco and G. Bertone, *Dynamical constraints on the dark matter distribution in the Milky Way*, *JCAP* **12** (2015) 001 [[1504.06324](#)].

[55] R. D. Peccei and H. R. Quinn, *CP Conservation in the Presence of Instantons*, *Phys. Rev. Lett.* **38** (1977) 1440.

[56] S. Weinberg, *A New Light Boson?*, *Phys. Rev. Lett.* **40** (1978) 223.

[57] F. Wilczek, *Problem of Strong P and T Invariance in the Presence of Instantons*, *Phys. Rev. Lett.* **40** (1978) 279.

[58] P.-H. Chavanis, *Mass-radius relation of Newtonian self-gravitating Bose-Einstein condensates with short-range interactions: I. Analytical results*, *Phys. Rev. D* **84** (2011) 043531 [[1103.2050](#)].

[59] E. D. Schiappacasse and M. P. Hertzberg, *Analysis of Dark Matter Axion Clumps with Spherical Symmetry*, *JCAP* **01** (2018) 037 [[1710.04729](#)].

[60] L. Visinelli, S. Baum, J. Redondo, K. Freese and F. Wilczek, *Dilute and dense axion stars*, *Phys. Lett. B* **777** (2018) 64 [[1710.08910](#)].

[61] P.-H. Chavanis, *Phase transitions between dilute and dense axion stars*, *Phys. Rev. D* **98** (2018) 023009 [[1710.06268](#)].

[62] P.-H. Chavanis, *Maximum mass of relativistic self-gravitating Bose-Einstein condensates with repulsive or attractive $-\varphi - 4$ self-interaction*, *Phys. Rev. D* **107** (2023) 103503 [[2211.13237](#)].

[63] H.-Y. Zhang, M. A. Amin, E. J. Copeland, P. M. Saffin and K. D. Lozanov, *Classical Decay Rates of Oscillons*, *JCAP* **07** (2020) 055 [[2004.01202](#)].

[64] H.-Y. Zhang, *Gravitational effects on oscillon lifetimes*, *JCAP* **03** (2021) 102 [[2011.11720](#)].

[65] D. G. Levkov, A. G. Panin and I. I. Tkachev, *Relativistic axions from collapsing Bose stars*, *Phys. Rev. Lett.* **118** (2017) 011301 [[1609.03611](#)].

[66] J. Fan, *Ultralight Repulsive Dark Matter and BEC*, *Phys. Dark Univ.* **14** (2016) 84 [[1603.06580](#)].

[67] H.-Y. Zhang and S. Ling, *Phenomenology of wavelike vector dark matter nonminimally coupled to gravity*, *JCAP* **07** (2023) 055 [[2305.03841](#)].

[68] N. D. Birrell and P. C. W. Davies, *Quantum Fields in Curved Space*, Cambridge Monographs on Mathematical Physics. Cambridge Univ. Press, Cambridge, UK, 2, 1984, [10.1017/CBO9780511622632](#).

[69] S. Weinberg, *The Quantum theory of fields. Vol. 1: Foundations*. Cambridge University Press, 6, 2005.

[70] C. G. Callan Jr, S. Coleman and R. Jackiw, *A new improved energy-momentum tensor*, *Annals of physics* **59** (1970) 42.

[71] D. Z. Freedman, I. J. Muzinich and E. J. Weinberg, *On the energy-momentum tensor in gauge field theories*, *Annals of Physics* **87** (1974) 95.

[72] D. Z. Freedman and E. J. Weinberg, *The energy-momentum tensor in scalar and gauge field theories*, *Annals of Physics* **87** (1974) 354.

[73] D. Ivanov and S. Liberati, *Testing Non-minimally Coupled BEC Dark Matter with Gravitational Waves*, *JCAP* **07** (2020) 065 [[1909.02368](#)].

[74] L. Ji, *Wave Dark Matter Non-minimally Coupled to Gravity*, [2106.11971](#).

[75] K. Sankharva and S. Sethi, *Nonminimally coupled ultralight axions as cold dark matter*, *Phys. Rev. D* **105** (2022) 103517 [[2110.04322](#)].

[76] B. Barman, N. Bernal, A. Das and R. Roshan, *Non-minimally coupled vector boson dark matter*, *JCAP* **01** (2022) 047 [[2108.13447](#)].

[77] A. A. Starobinsky, *Spectrum of relict gravitational radiation and the early state of the universe*, *JETP Lett.* **30** (1979) 682.

[78] M. S. Turner and L. M. Widrow, *Inflation Produced, Large Scale Magnetic Fields*, *Phys. Rev. D* **37** (1988) 2743.

[79] L. H. Ford, *INFLATION DRIVEN BY A VECTOR FIELD*, *Phys. Rev. D* **40** (1989) 967.

[80] V. Faraoni, *Inflation and quintessence with nonminimal coupling*, *Phys. Rev. D* **62** (2000) 023504 [[gr-qc/0002091](#)].

[81] A. Golovnev, V. Mukhanov and V. Vanchurin, *Vector Inflation*, *JCAP* **06** (2008) 009 [[0802.2068](#)].

[82] A. Golovnev, V. Mukhanov and V. Vanchurin, *Gravitational waves in vector inflation*, *JCAP* **11** (2008) 018 [[0810.4304](#)].

[83] A. Golovnev and V. Vanchurin, *Cosmological perturbations from vector inflation*, *Phys. Rev. D* **79** (2009) 103524 [[0903.2977](#)].

[84] A. Golovnev, *Linear perturbations in vector inflation and stability issues*, *Phys. Rev. D* **81** (2010) 023514 [[0910.0173](#)].

[85] J. W. Moffat, *Scalar-tensor-vector gravity theory*, *JCAP* **03** (2006) 004 [[gr-qc/0506021](#)].

[86] J. R. Brownstein and J. W. Moffat, *Galaxy rotation curves without non-baryonic dark matter*, *Astrophys. J.* **636** (2006) 721 [[astro-ph/0506370](#)].

[87] G. Tasinato, *Cosmic Acceleration from Abelian Symmetry Breaking*, *JHEP* **04** (2014) 067 [[1402.6450](#)].

[88] L. Heisenberg, *Generalization of the Proca Action*, *JCAP* **05** (2014) 015 [[1402.7026](#)].

[89] A. De Felice, L. Heisenberg, R. Kase, S. Mukohyama, S. Tsujikawa and Y.-l. Zhang, *Cosmology in generalized Proca theories*, *JCAP* **06** (2016) 048 [[1603.05806](#)].

[90] A. de Felice, L. Heisenberg and S. Tsujikawa, *Observational constraints on generalized Proca theories*, *Phys. Rev. D* **95** (2017) 123540 [[1703.09573](#)].

[91] B. Salehian, H.-Y. Zhang, M. A. Amin, D. I. Kaiser and M. H. Namjoo, *Beyond Schrödinger-Poisson: nonrelativistic effective field theory for scalar dark matter*, *JHEP* **09** (2021) 050 [[2104.10128](#)].

[92] X. Du, B. Schwabe, J. C. Niemeyer and D. Bürger, *Tidal disruption of fuzzy dark matter subhalo cores*, *Phys. Rev. D* **97** (2018) 063507 [[1801.04864](#)].

[93] J. Chen, L. H. Nguyen, X. Du and D. J. E. Marsh, *Vector Dark Matter Halo: From Polarization Dynamics to Direct Detection*, [2407.17315](#).

[94] J. Chen, *Simulations of Bosonic Dark Matter*, Ph.D. thesis, Gottingen U., Gottingen, U., 2021. 10.53846/goediss-8928.

[95] T. Lee and Y. Pang, *Nontopological solitons*, *Phys. Rept.* **221** (1992) 251.

[96] H.-Y. Zhang, *Probing ultralight dark fields in cosmological and astrophysical systems*, Ph.D. thesis, Rice U., 2023. [2401.00043](#).

[97] J. Chen, X. Du, E. W. Lentz and D. J. E. Marsh, *Relaxation times for bose-einstein condensation by self-interaction and gravity*, *Phys. Rev. D* **106** (2022) 023009.

[98] P. Mocz et al., *Cosmological structure formation and soliton phase transition in fuzzy dark matter with axion self-interactions*, *Mon. Not. Roy. Astron. Soc.* **521** (2023) 2608 [[2301.10266](#)].

[99] K. Fujikura, M. P. Hertzberg, E. D. Schiappacasse and M. Yamaguchi, *Microlensing constraints on axion stars including finite lens and source size effects*, *Phys. Rev. D* **104** (2021) 123012 [[2109.04283](#)].

[100] N. Dalal and A. Kravtsov, *Excluding fuzzy dark matter with sizes and stellar kinematics of ultrafaint dwarf galaxies*, *Phys. Rev. D* **106** (2022) 063517 [[2203.05750](#)].

[101] B. Eggemeier, C. A. J. O’Hare, G. Pierobon, J. Redondo and Y. Y. Y. Wong, *Axion minivoids and implications for direct detection*, *Phys. Rev. D* **107** (2023) 083510 [[2212.00560](#)].